

JPL PUBLICATION 85-82

Characterization of EMI Generated by the Discharge of a "VOLT" Solar Array

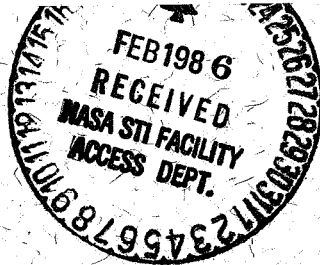
Final Report

Philip Leung

{NASA-CR-176537} CHARACTERIZATION OF EMI
GENERATED BY THE DISCHARGE OF A VOLT SOLAR
ARRAY Final Report (Jet Propulsion Lab.)
24 p HC A03/MF A01 CSCL 10A

N86-19740

G3/44 05460
Unclas



November 1, 1985

NASA

National Aeronautics and
Space Administration

Jet Propulsion Laboratory
California Institute of Technology
Pasadena, California

JPL PUBLICATION 85-82

Characterization of EMI Generated by the Discharge of a "VOLT" Solar Array

Final Report

Philip Leung

November 1, 1985

NASA

National Aeronautics and
Space Administration

Jet Propulsion Laboratory
California Institute of Technology
Pasadena, California

The research described in this publication was carried out by the Jet Propulsion Laboratory, California Institute of Technology, under a contract with the National Aeronautics and Space Administration.

Reference herein to any specific commercial product, process, or service by trade name, trademark, manufacturer, or otherwise, does not constitute or imply its endorsement by the United States Government or the Jet Propulsion Laboratory, California Institute of Technology.

ABSTRACT

The interaction of a high-voltage solar array with the space plasma environment is investigated in a laboratory simulation experiment. Discharges are observed to occur when the solar array is at a sufficiently high negative bias with respect to the plasma. The frequency of occurrence of discharge is found to depend critically on the plasma density and on the geometry of the array. The electromagnetic interference (EMI) associated with a discharge is also measured. The amplitude of EMI increases with the magnitude of the high voltage. Since the discharge-generated EMI is of significant amplitude, its effect on the performance of systems in space must be evaluated.

CONTENTS

I.	INTRODUCTION	1
II.	EXPERIMENTAL SETUP	1
A.	Plasma Source	3
B.	The Solar Array Sample	5
C.	Diagnostic Instruments for Measuring Discharge Characteristics	8
III.	EXPERIMENTAL RESULTS	11
A.	Discharge Rate Measurements	11
B.	RF Radiation Measurements	14
C.	Conducted Emissions	14
IV.	SUMMARY	17
	REFERENCES	18

Figures

1.	Schematic of the experimental setup	2
2.	Schematics of the synthesis plasma source: (a) The electron emitter is an indirectly heated cathode. (b) The electron emitter is made of tungsten wires.	4
3.	A typical Langmuir probe I-V trace	6
4.	The "PIX" array: (a) photograph, (b) test configuration	7
5.	The "VOLT" array: (a) photograph, (b) test configuration	9
6.	Schematic of the pulse counting circuit	10
7.	Discharge rate as a function of biased voltage	12
8.	Discharge rate as a function of plasma density	12
9.	The spectra of RF radiation generated by a discharge. The biased voltage is 1000 V.	15
10.	The spectra of RF radiation as a function of the biased voltage	15
11.	The spectra of RF radiation generated by the "VOLT" array with and without an external capacitor	16
12.	A typical capacitive probe signal. The bias on the "VOLT" array is 626 V.	16

CONTENTS (Continued)

Tables

1.	Plasma parameters produced by the synthesis plasma source	5
2.	Operating conditions for the electron and ion sources	5
3.	Summary of "PIX" array discharge rate measurements	13
4.	Summary of "VOLT" array discharge rate measurements	13

I. INTRODUCTION

Future space missions will require very large, high-power spacecraft for use in near-earth-orbit missions. To meet this need, 100-kW space power systems are being developed using high-voltage solar arrays. However, previous experiments¹⁻⁴ have shown that discharges are generated in the interaction of a high-voltage array with an ambient plasma. Discharges are undesirable because the electromagnetic interference (EMI) generated during a discharge may cause temporary or even permanent disruption in the operation of spacecraft systems. Consequently, the occurrence of discharges may be the limiting factor in the operating voltage of a high-voltage array. The Plasma Interaction Experiment (PIX) II flight experiment, which was designed and managed by NASA Lewis Research center, has verified the occurrence of the discharge phenomenon in low-earth orbits.⁵

Lewis Research Center is currently developing the Voltage Operating Limit Tests (VOLT) experiment to further investigate the interaction of high-voltage solar arrays with the space plasma environment. The VOLT experiment will be performed on the Shuttle. It is expected that discharges will occur during the VOLT experiments. In order to predict the adverse effects of these discharges on the shuttle and its payload, it is essential that the magnitude of the discharge-generated EMI be determined through ground tests. For this reason, a ground-based laboratory program to investigate the interaction of a high-voltage array with an ambient plasma has been carried out. The objectives of this investigation are as follows:

- (1) To determine the discharge rate as a function of the high-voltage bias on the solar array and as a function of the plasma density.
- (2) To characterize the radiofrequency radiation (RF) generated during a discharge event.

The results of this investigation are presented below.

II. EXPERIMENTAL SETUP

Figure 1 shows the experimental setup, which has three essential components:

- (1) The plasma source
- (2) The solar array sample
- (3) The diagnostic for measuring the transient current and the RF radiation

The plasma source and the solar array sample are installed inside a vacuum chamber. For this investigation, a large vacuum chamber with acrylic walls is used. Since acrylic is transparent to RF, the observed RF characteristics will not be dominated by cavity effects. The details of this acrylic facility are discussed in a previous publication.⁶

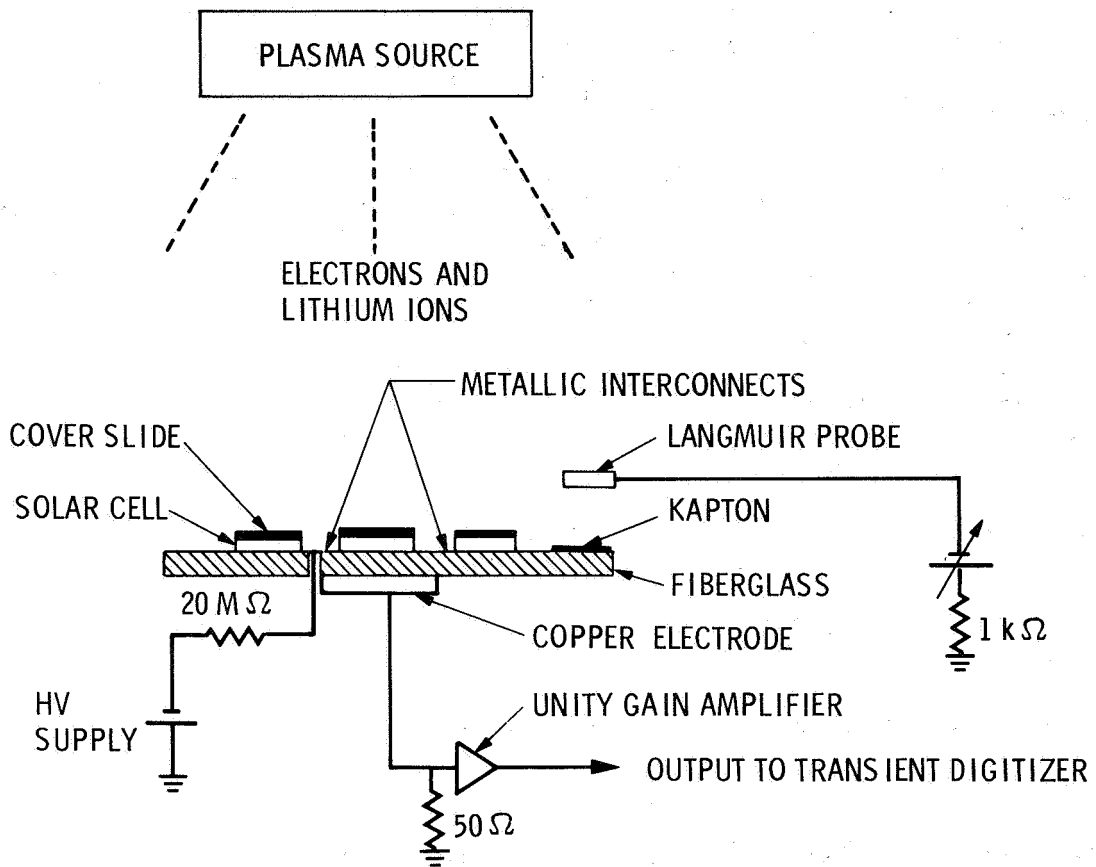


Figure 1. Schematic of the experimental setup

A. Plasma Source

Since the emphasis of this investigation is the discharge phenomenon and the characterization of discharge-generated EMI, severe restrictions are imposed on the experimental setup, particularly on the plasma source. In order to achieve the objectives, the plasma source must satisfy the following requirements:

- (1) It must not be a source of EMI.
- (2) It must be capable of operating at low neutral pressure ($< 10^{-5}$ torr).
- (3) It must be capable of generating a plasma with a density of $10^5/\text{cm}^3$ or higher.

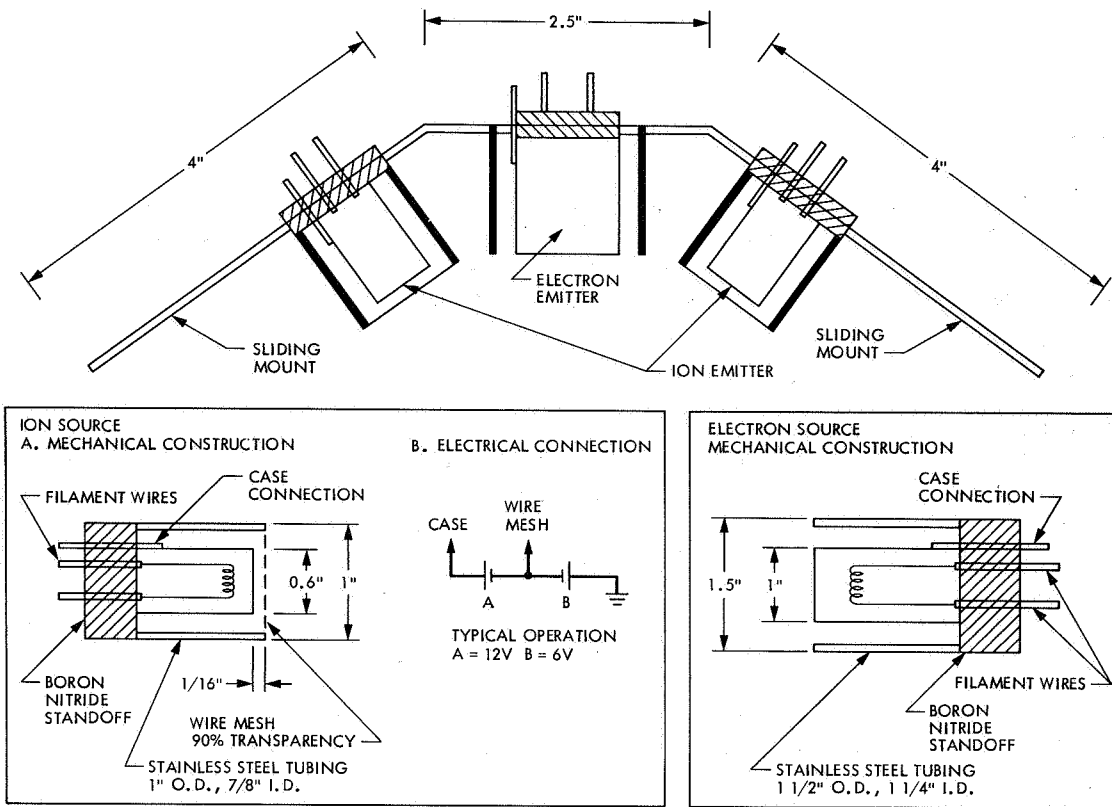
The most common plasma sources, such as an ion thruster plasma source, use gaseous discharge to generate a plasma. This type of plasma source is not suitable for this investigation because of the following reasons:

- (1) A high neutral pressure is required for its operation.
- (2) The EMI level associated with a discharge source is usually much higher than the ambient EMI level.

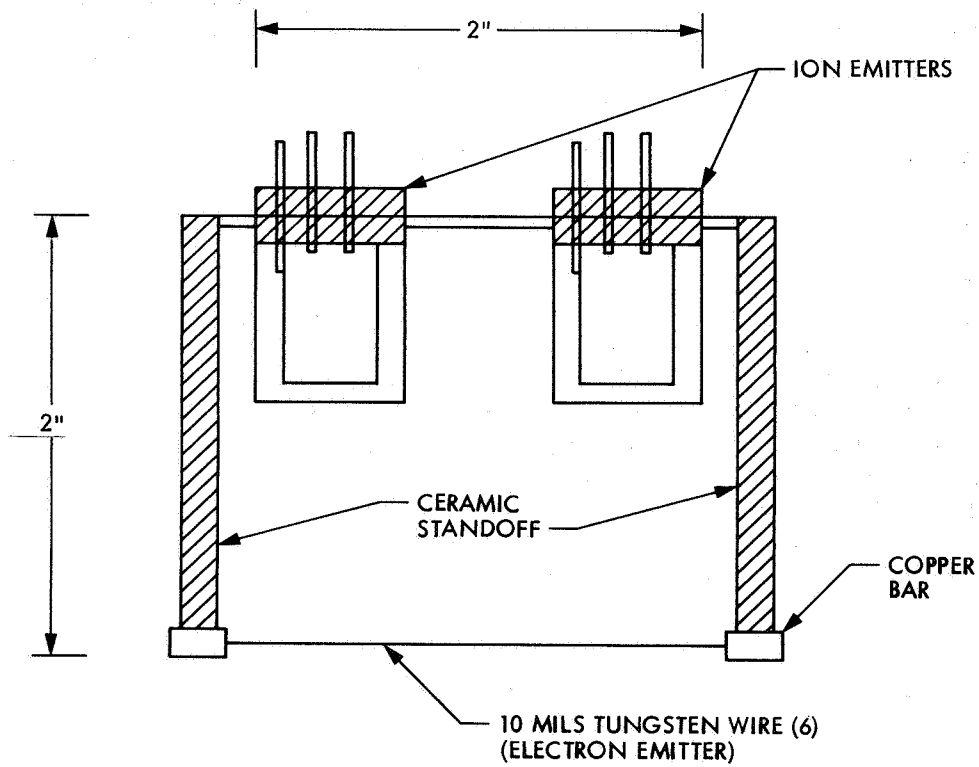
Therefore, the investigators developed a novel plasma source that is basically a synthesis plasma source, consisting of separate electron and ion emitters. The ion emitter is a β -eucryptite source that emits lithium (Li^7) ions; the electron emitter is an oxide-coated cathode or tungsten filaments. Figures 2a and 2b show two different configurations of this synthesis plasma source. These two configurations differ by their electron emitters.

The ion sources in both plasma configurations are identical. The potential difference between the grid and the case controls the ion current. The ion energy is determined by the potential of the case with respect to ground.

In a typical operation, the electron source is electrically grounded. That is, the case of the cathode (figure 2a) or the filaments (figure 2b) is connected to ground. The presence of the ions creates a positive space potential in the vicinity of the electron source. The resulting electric field enhances the emission of the electron source, creating a high-density plasma. The observed enhancement factor of electron emission is in the range of 5 to 10. Table 1 shows the plasma parameters obtained with this synthesis plasma source. The higher electron temperature is obtained with the configuration shown in figure 2b. The electron temperature of this configuration is in the range of 3 eV and is attributed to the potential drop across the filaments.



(a)



(b)

Figure 2. Schematics of the synthesis plasma source: (a) The electron emitter is an indirectly heated cathode. (b) The electron emitter is made of tungsten wires.

Table 1. Plasma parameters produced by the synthesis plasma source

Condition	Plasma Density (particles/cm ³)	Electron Temperature (eV)	Ion Energy (eV)
Optimum	5 x 10 ⁶	0.8	6
Typical	6 x 10 ⁵	0.8 to 3	6 to 12

Table 2 shows the power requirement for the plasma sources. Since the operation of this synthesis plasma source does not require neutral gas, the vacuum pressure during its operation is usually at the background level. For the vacuum facility used in this experiment, this pressure level is in the range of 10⁻⁶ torr.

Table 2. Operating conditions for the electron and ion sources

Source	Heater Voltage (V)	Heater Current (A)
Ion Source	12	8.5
Cathode Electron Emitter	12	15
Tungsten Wire (6 x 10 mils)	4	7/wire

A Langmuir probe is used to characterize the electron temperature and the plasma density. Figure 3 shows a typical Langmuir probe I-V curve obtained in this experimental setup. In most cases, a distinct saturation region for the electron current (knee) can be identified. The Langmuir trace of figure 3 shows that the electron distribution of this synthesis plasma source is nearly thermal. The design of this source precludes the existence of energetic electrons (electron beam); for this reason, electrostatic instabilities⁷ are not excited in this plasma. Consequently, the EMI level of the plasma generated by this source is at the ambient level.

B. The Solar Array Sample

Two solar arrays with different geometries are used in this experiment.

- (1) One array has twenty-four 2-cm by 2-cm solar cells. This array is similar to the arrays used in the PIX program^{5,8} and is herein referred to as the "PIX" array. A picture of this array is shown in figure 4a; the electrical connections are shown in figure 4b.

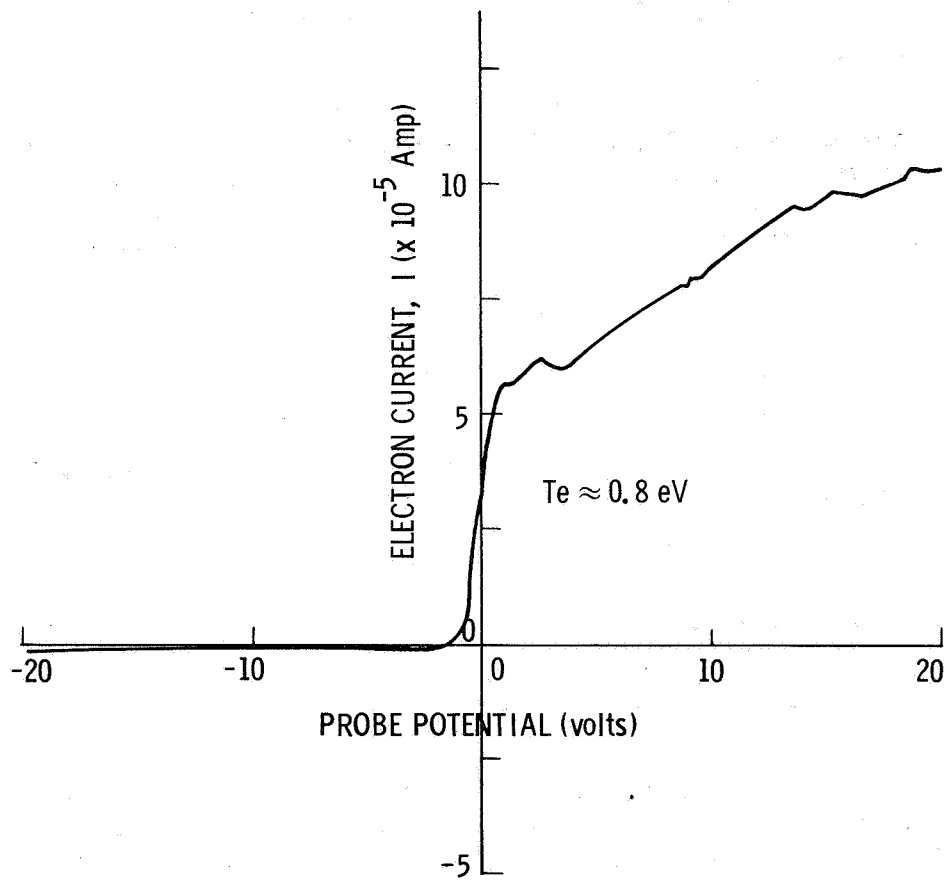
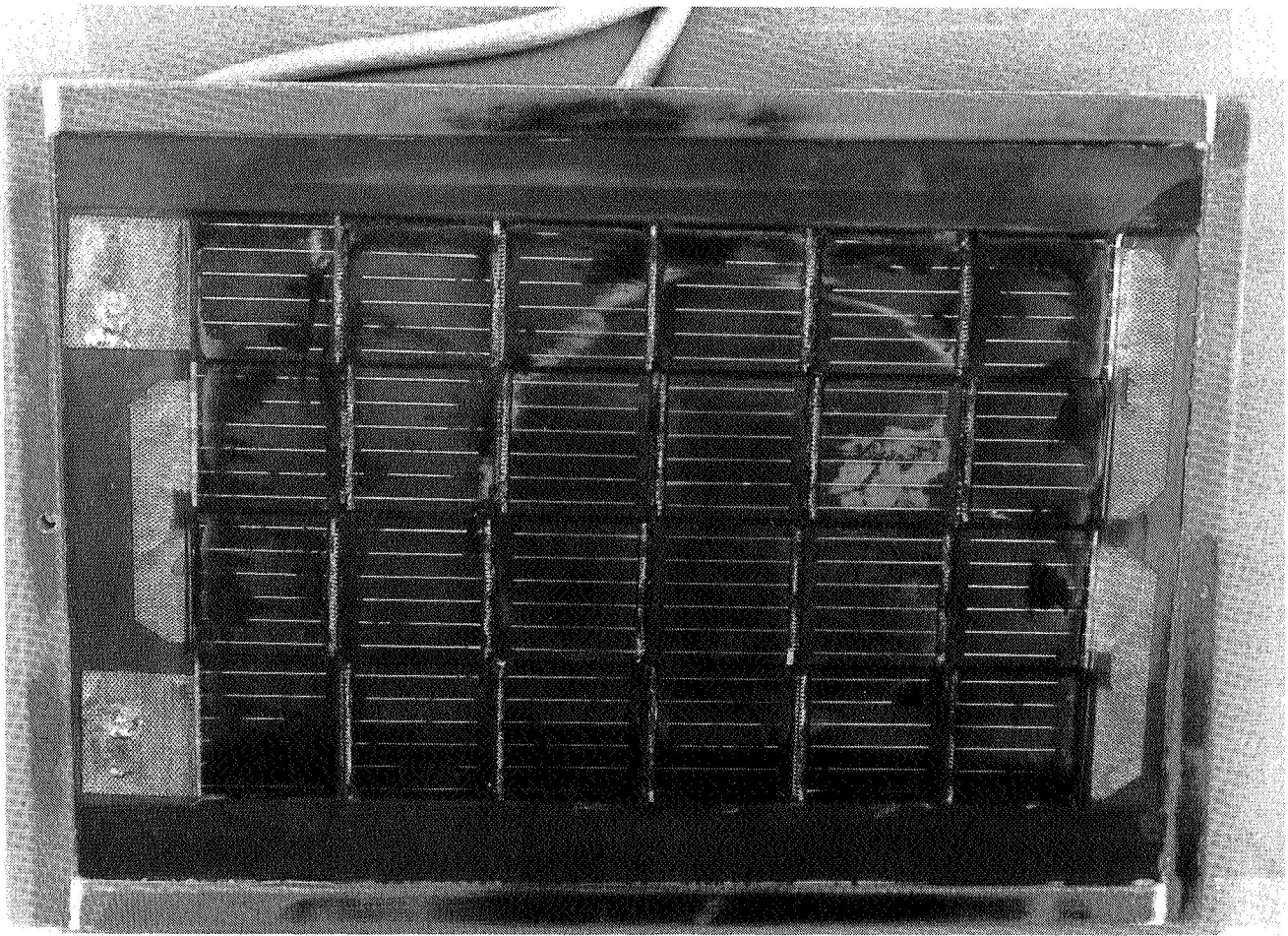
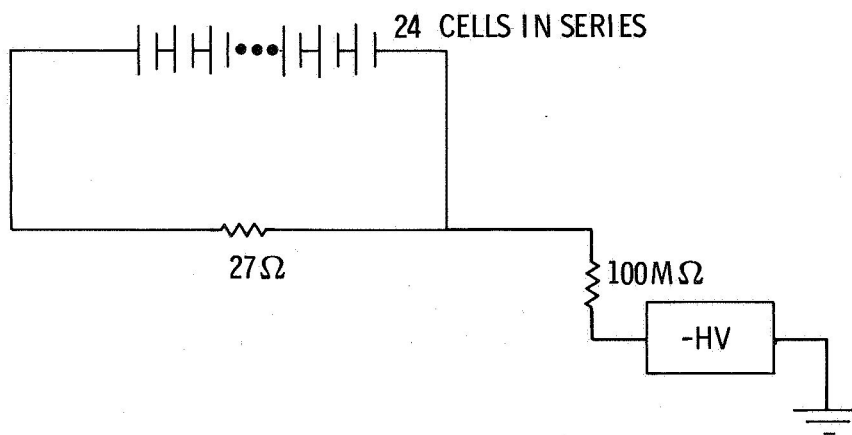


Figure 3. A typical Langmuir probe I-V trace



(a)



(b)

Figure 4. The "PIX" array: (a) photograph, (b) test configuration

- (2) The second array has four 5.9-cm by 5.9-cm solar cells (figure 5a). This array is similar to the array used in the VOLT program,⁹ and is herein referred to as the "VOLT" array. The electrical connection of this array is shown in figure 5b.

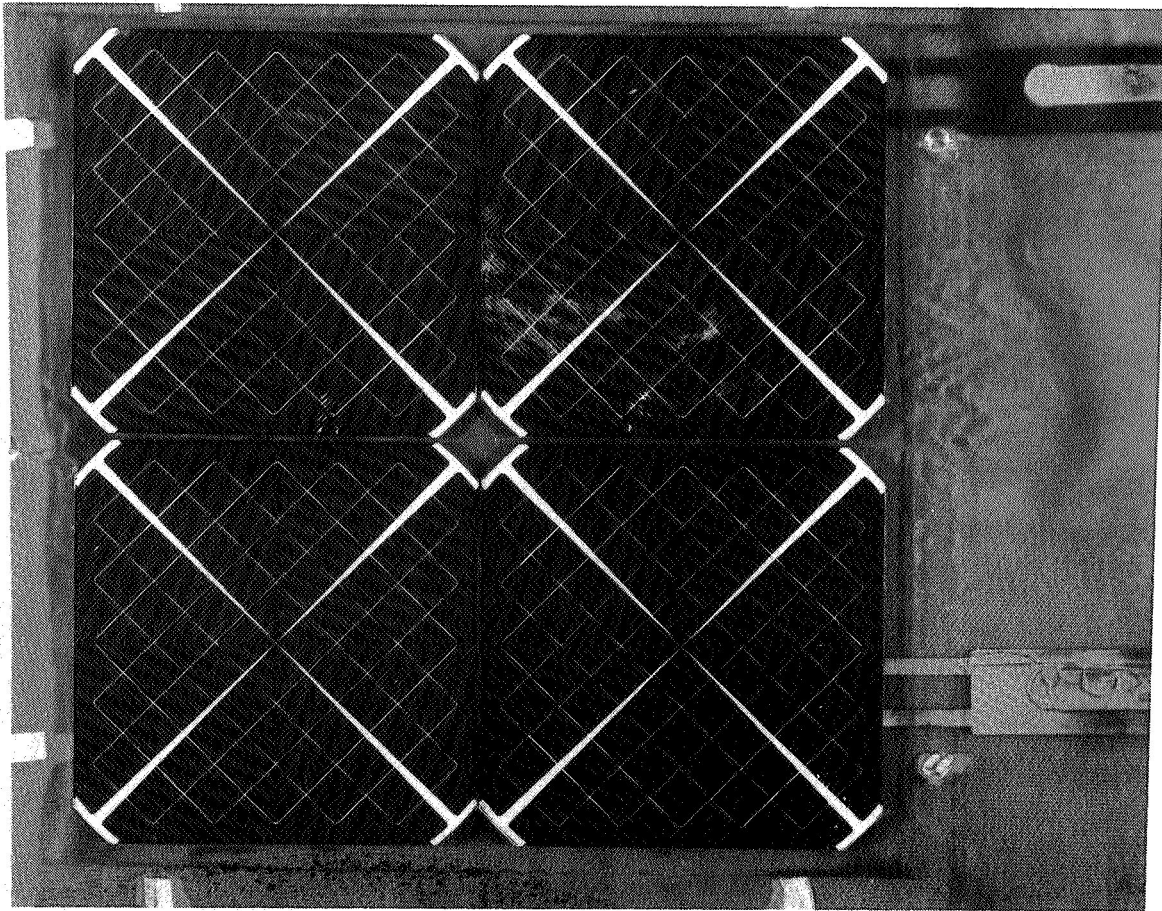
In each array, a fused silica cover slide is placed on top of each solar cell and the cells are electrically connected in series with the solar cells. The area of each array is approximately 100 cm². Each array is mounted on a fiberglass board. To simulate a high-voltage solar array, a high-voltage bias is applied to the interconnects. Since previous experiments¹⁻⁴ have shown that discharges only occur when the solar array is at a negative potential, all the experiments in this investigation are performed with a negatively biased array.

C. Diagnostic Instruments for Measuring Discharge Characteristics

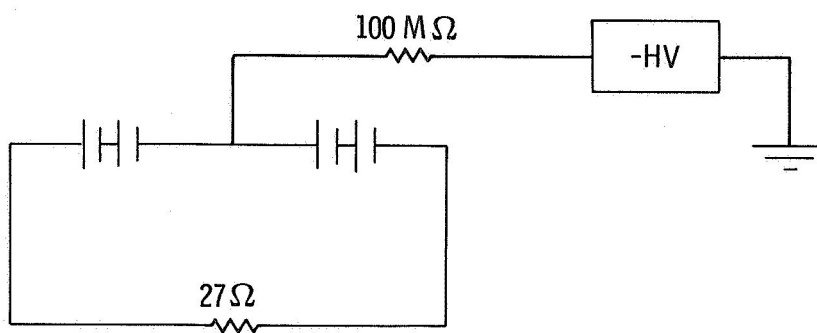
A capacitive probe is constructed by attaching a copper electrode to the back of the fiberglass board on which the solar array is mounted. When a discharge occurs, the potential at the interconnect drops, and a fast transient signal is coupled to the probe. The signal detected by the capacitive probe is processed by a fast time response voltage follower circuit.³ The capacitance of the capacitive probe ranges from 5 pF to 25 pF. The input impedance of the follower circuit is 50 Ω ; therefore, the follower circuit has a maximum RC time constant of 1.25 ns. The signal from the follower circuit is digitized and stored on a disk for later analysis. The time integral of this signal provides information on the voltage drop (charge loss) during a discharge.³ To avoid the effect of the stray capacitance due to the cables, the follower circuit is placed inside the vacuum chamber and is installed directly underneath the solar array.

In order to determine the rate of discharges, a pulse counting circuit is developed. Figure 6 shows a schematic of this circuit. In this circuit, the sensitivity of the 7A26 amplifier and the trigger level of the scope acts as a discriminator for the discharge pulse. Previous experiments³ have shown that discharges of various amplitudes are generated during the discharge of a solar array. For each biased voltage, the level of the discriminator is set such that only discharges of significant size will be registered, i.e., discharges that produce a voltage drop of >30% of the applied high voltage. The results of discharge rate measurements presented in this paper are derived from data on large amplitude discharges.

The RF radiation generated during a discharge is measured by antennas with different frequency responses. In the frequency range of 0.1 MHz to 40 MHz, the radiated signal is measured, for redundancy, by two monopole antennas: the Singer 95010 and the Empire VA-105. These antennas have receivers with different bandwidths. The Singer antenna system has a flat frequency response from 0.04 MHz to 40 MHz. The signal from this antenna is digitized and stored on a disk. During the data reduction process, the frequency spectrum of RF radiation is obtained with a Fourier transform of the time domain signal. The Empire VA-105 antenna system has a narrower bandwidth. The receiver is of resonant-type LC circuit and has six selectable frequency bands, spaced logarithmically. The bandwidth of each frequency band is approximately equal to



(a)



(b)

Figure 5. The "VOLT" array: (a) photograph, (b) test configuration

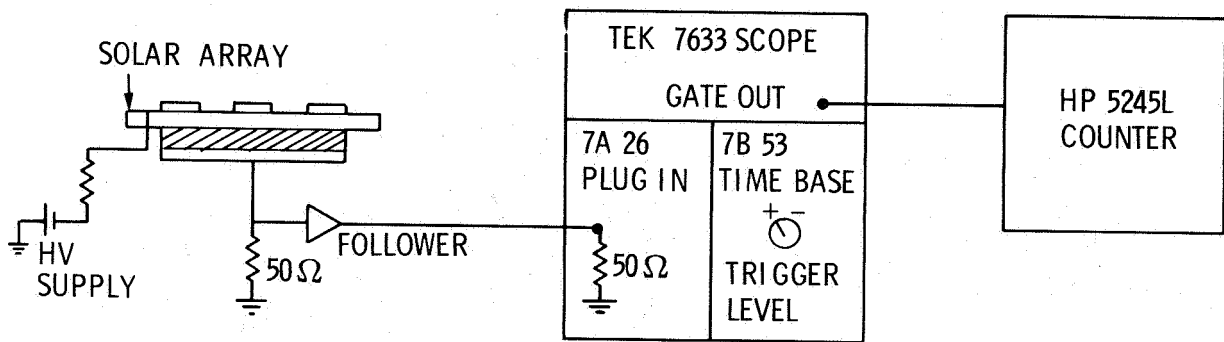


Figure 6. Schematic of the pulse counting circuit

the center frequency. The RF spectra derived from these two instruments agree well (± 3 db). The RF radiation in the frequency range 30 to 200 MHz is measured by a biconical antenna (EMCO 3104), and the RF radiation in the frequency range of 200 to 1000 MHz is measured by a log-conical antenna (EMCO 3101). The signals from these antennas are processed by detectors with bandwidths ranging from 100 to 300 MHz.

III. EXPERIMENTAL RESULTS

A. Discharge Rate Measurements

Discharges are observed on a negatively biased solar array under various plasma conditions. Figure 7 shows the discharge rate as a function of the bias voltage for a plasma density of $5 \times 10^5/\text{cm}^3$. This is the typical density encountered in low-earth orbits. Under the same condition, the discharge rate for the "PIX"-type array is about an order of magnitude higher than that for the "VOLT"-type array.

There is a significant difference between the geometries of the interconnects of the "VOLT" and "PIX" arrays. The interconnects of the "PIX" array are made of braided conductors and are directly exposed to the plasma environment. The interconnects of the "VOLT" array are of "wraparound type" and are not exposed to the outside environment. Although the areas of both arrays are approximately equal, the area of exposed interconnects is much higher for the "PIX" array. Visual inspection also indicates that the braided conductor of the "PIX" array has much sharper geometries than the "VOLT"-type array. The drastic difference in the geometries of these two arrays probably accounts for the difference in the observed discharge rates.

The effect of the plasma density on the "PIX" array is illustrated in figure 8. The bias on the array is 626 V. The data indicate that there is a threshold plasma density at which a discharge occurs; for the "PIX" array, this density is approximately $10^4/\text{cm}^3$. Above the threshold density, the discharge rate increases rapidly.

A summary of the discharge rate measurements is presented in Tables 3 and 4. The variables in these tables are the plasma density and the biased voltage. The numerical values in the tables are the discharge rates; a discharge rate of zero means no discharge was observed during the experiment. The minimum time interval of the experiment is 20 minutes. In boxes where there are no entries, no experiment was performed under those conditions. With a few exceptions, the expected discharge rate corresponding to the no-entry boxes is zero. By comparing the data in tables 3 and 4, it is obvious that the "PIX" array is more prone to discharge.

The data displayed in figures 7 and 8 and tables 3 and 4 were obtained within two hours after the commencement of each experiment; the discharge rate decreases after an extended experimentation time. For example, the discharge rate measured two hours after the start of the experiment can be 3 times lower than the discharge rate measured at the beginning of the experiment. The magnitude of the capacitive probe signal and the RF radiation are not affected by time.

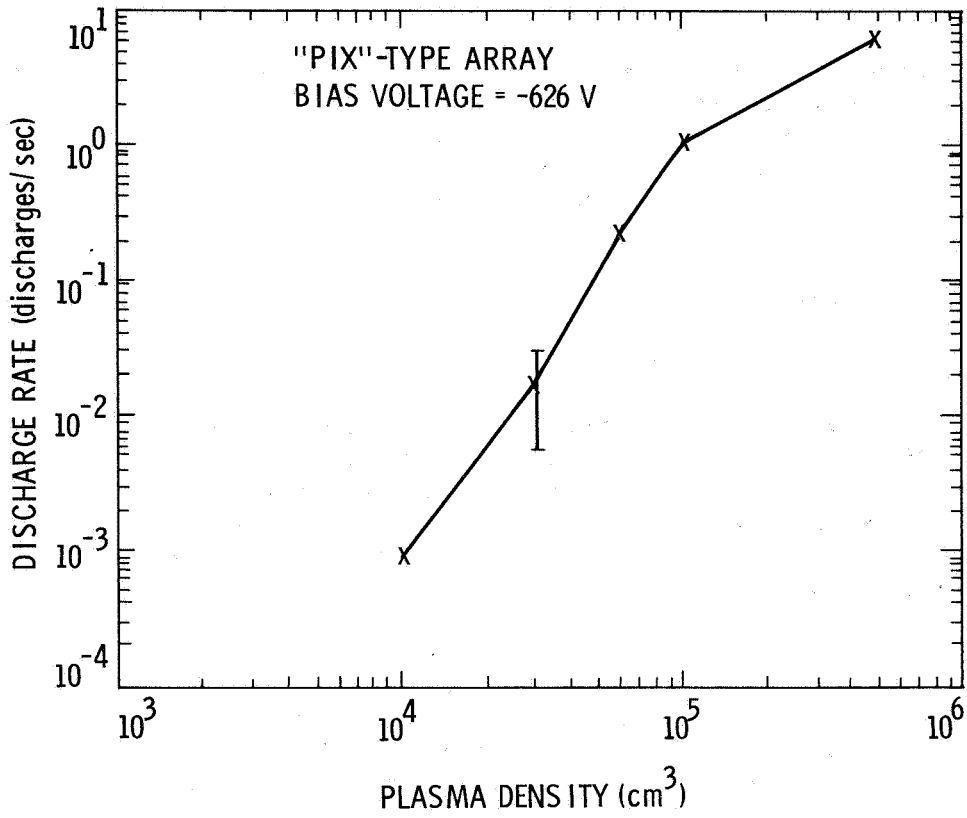


Figure 7. Discharge rate as a function of biased voltage

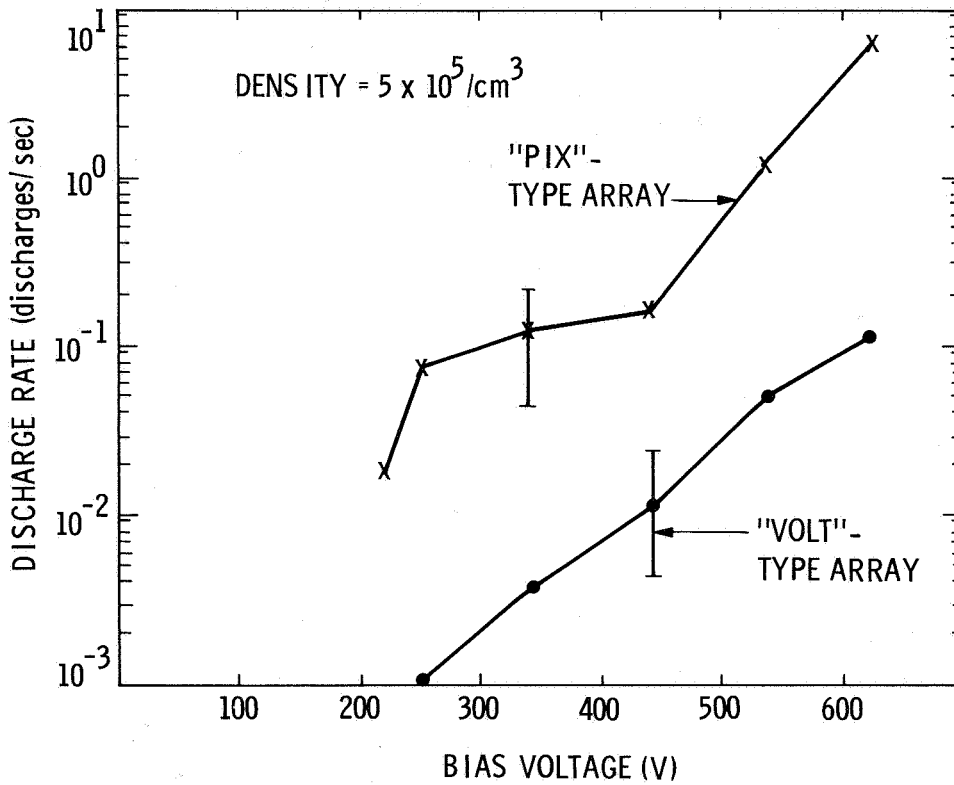


Figure 8. Discharge rate as a function of plasma density

Table 3. Summary of "PIX" array discharge rate measurements
(discharge rate in discharges/sec)

Bias Voltage (V)	Plasma Density (particles/cm ³)				
	6 x 10 ⁵	10 ⁵	6 x 10 ⁴	3 x 10 ⁴	10 ⁴
626	6.2	1.2	0.23	0.02	0.0009
532	1.3	0.15	0.02	---	0
438	0.15	---	0.005	---	0
344	0.12	---	0	---	0
250	0.08	---	0	---	0
218	0.017	---	0	---	0

Table 4. Summary of "VOLT" array discharge rate measurement
(discharge rate in discharges/sec)

Bias Voltage (V)	Plasma Density (particles/cm ³)				
	6 x 10 ⁵	10 ⁵	6 x 10 ⁴	3 x 10 ⁴	10 ⁴
626	0.13	0.017	0	0	0
532	0.05	0.005	0	0	0
438	0.012	0	---	---	---
344	0.004	---	---	---	---
250	0.001	---	---	---	---
218	0	---	---	---	---

B. RF Radiation Measurements

High-frequency electromagnetic radiation is generated by a discharge of a solar array. A measurement of the amplitude of the RF radiation as a function of distance shows that the radiation emitted by a discharge roughly resembles the radiation emitted by a dipole. The amplitude (E) decreases with the distance (r) as

$$E \propto 1/r^n \quad (1)$$

where n is in the range of 2 to 3. The average value for n is 2.5.

Figure 9 displays the spectra of RF radiation generated during discharges for the "PIX" and the "VOLT" arrays. The data were obtained with a biased voltage of 1000 V and were obtained during discharges of significant magnitudes.³ Due to the size of the vacuum system, the antennas were placed at a distance of 2 to 4 m from the solar arrays. The data displayed in figure 9 are the RF electric field at a distance of 1 m from the solar array. Their numerical values are extrapolated from measured data using equation 1, with n = 2.5. The error bars show the uncertainty introduced by the extrapolation process. The amplitudes of RF radiation generated by the discharge of both arrays are approximately the same. In order to illustrate the effect of discharge-generated RF on spaceflights, the levels of RF radiation¹⁰ allowed for the space shuttle are also displayed on figure 9.

Figure 10 shows the dependence of the RF radiation on the biased voltage. The amplitude is a nonlinear function of the biased voltage. In a typical discharge, the transient current involved in a discharge is proportional to the amount of charge lost in a discharge; consequently, the amplitude of RF radiation increases with the voltage bias. Experimental observation indicates that when the biased voltage is at 626 and 1000 V, approximately 80 to 100% of the stored charge is released during a discharge. However, at a biased voltage of 250 V, only 30 to 40% of the stored charge is released. Therefore, the observed amplitude of the discharge generated RF is a nonlinear function of the biased voltage.

The test samples in this experiment are small solar arrays. In a large solar array, the capacitance between the interconnects and the ground structure is substantially larger, and the resulting discharge may have a higher amplitude. In an attempt to simulate the effect of discharge of a large solar array, a 2000-pF capacitor was connected between the interconnect of a "VOLT" array and the ground structure. Figure 11 shows the resulting data; in the presence of the 2000 pF capacitor, the measured electric field is 20 dB higher.

C. Conducted Emissions

Due to the large limiting resistor (100 M Ω) in the high-voltage supply circuit in the test configuration, the main source of conducted noise is derived from capacitive coupling between the array and a possible victim circuit. That is, the transient current that can be coupled into circuits is proportional to dV/dt. The value of dV/dt can be derived from the signals of the capacitive probe. Figure 12 shows a typical signal detected by the capacitive probe during a discharge event. If the surface voltage of the

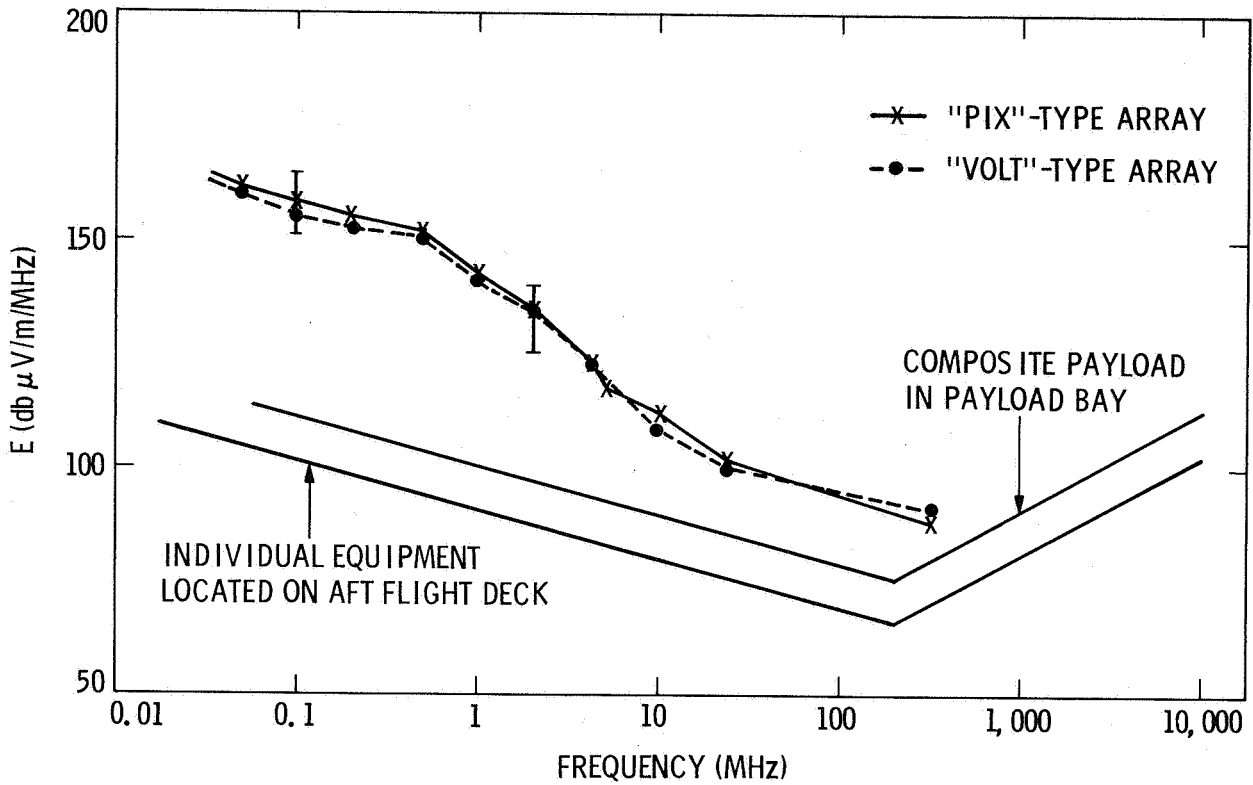


Figure 9. The spectra of RF radiation generated by a discharge. The biased voltage is 1000 V.

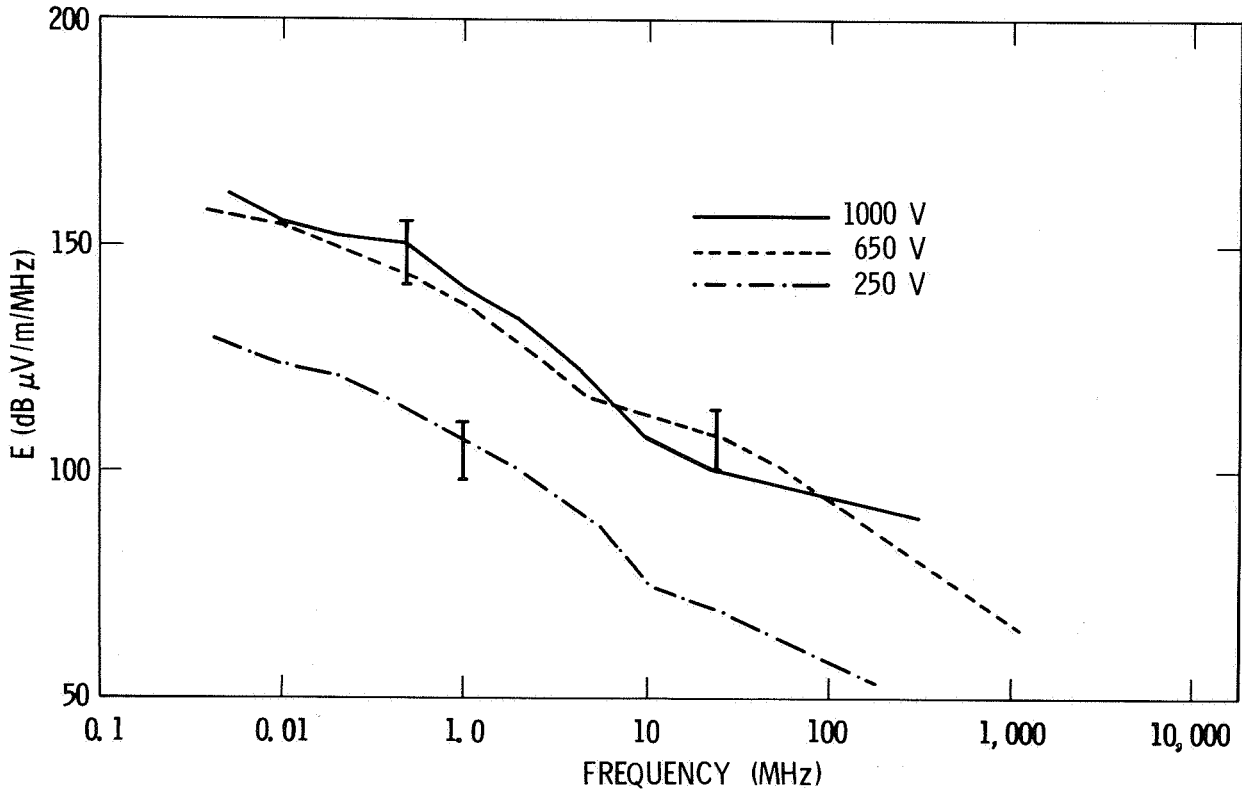


Figure 10. The spectra of RF radiation as a function of the biased voltage

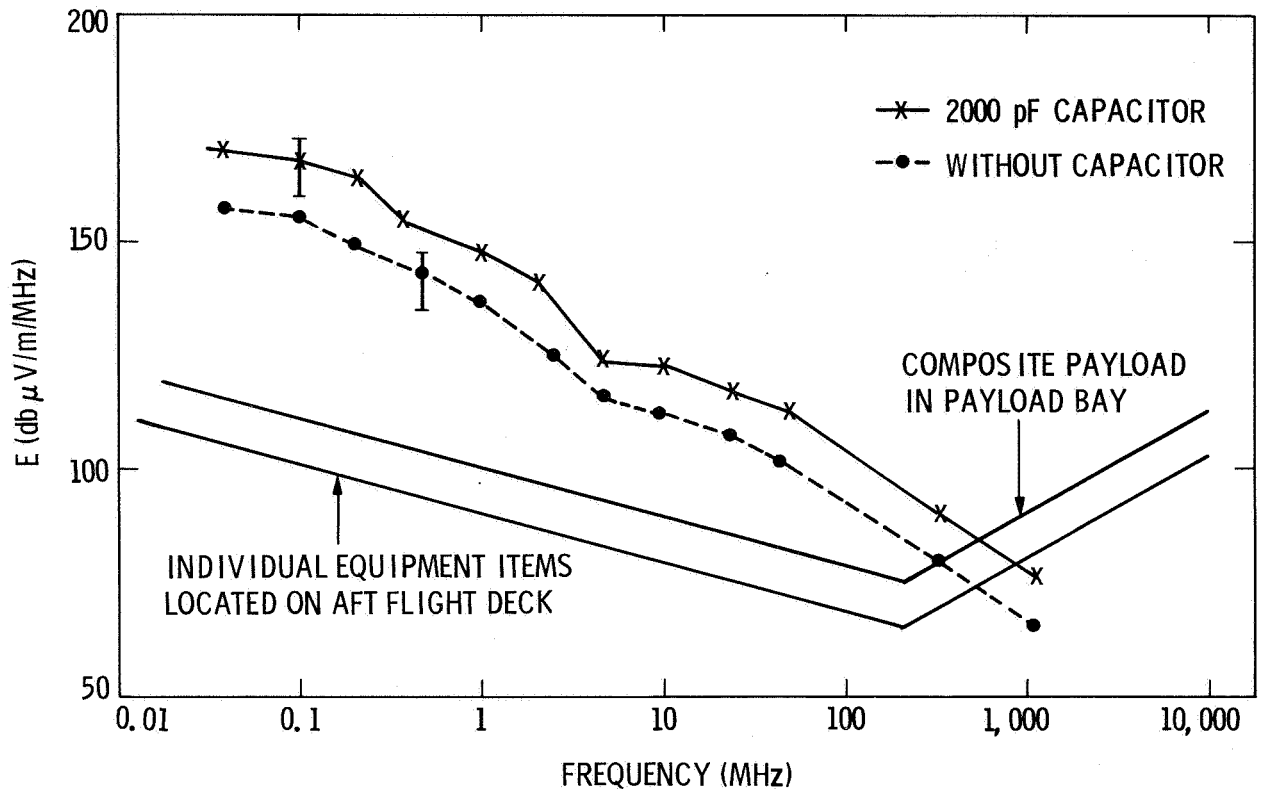


Figure 11. The spectra of RF radiation generated by the "VOLT" array with and without an external capacitor

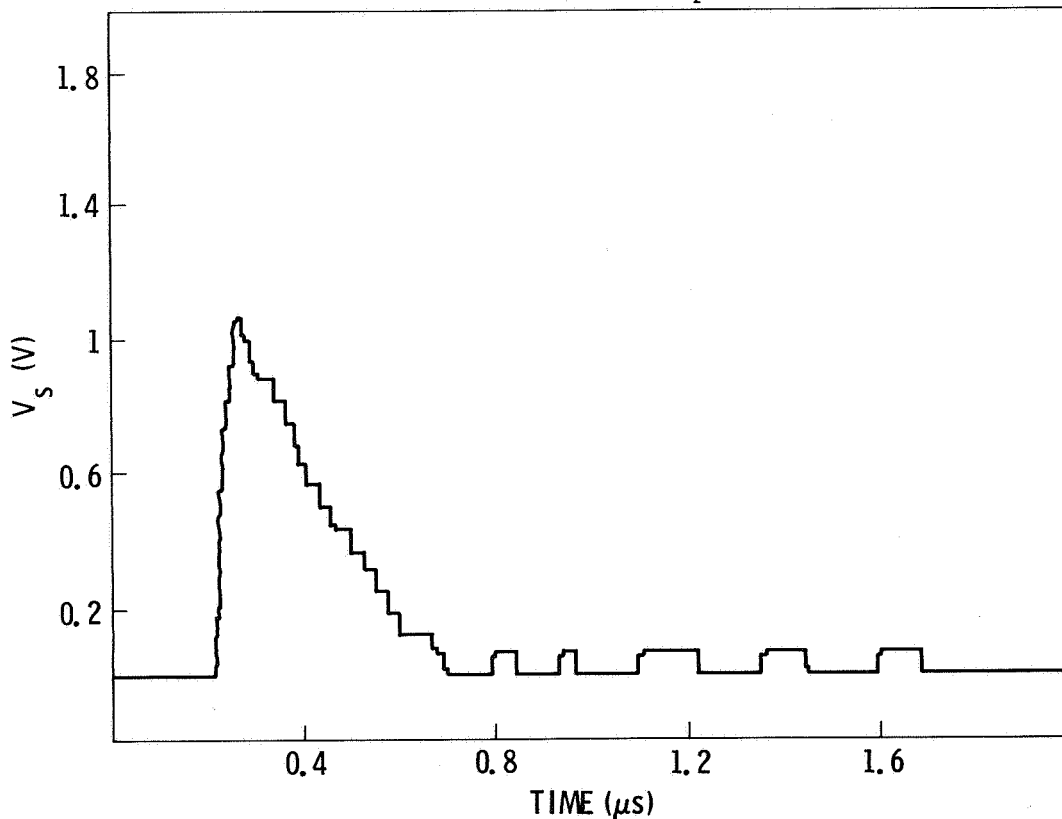


Figure 12. A typical capacitive probe signal. The bias on the "VOLT" array is 626 V.

cover-slides remains unchanged during a discharge event, the value of dV/dt can be derived from the following equation:

$$dV/dt = V_s/RC \quad (2)$$

where V_s is the capacitive signal, R is the input impedance of the follower circuit, and C is the capacitance of the capacitive probe. For the "VOLT" array, R is 50Ω and C is 7.5 pF . The data in figure 10 show that the peak value of dV/dt is $2.7 \times 10^9 \text{ V/s}$.

The transient current (I) that can be coupled into a nearby circuit is given by:

$$I = C dV/dt \quad (3)$$

where C is the capacitance between the array and the victim circuit. The above equation is only valid if C is smaller than the capacitance between the array and ground (this condition is usually satisfied.) The "VOLT" array has a capacitance of 30 pF with respect to ground; the data in figure 10 indicate that the maximum current that can be coupled to a unshielded victim circuit is 0.08 A . The waveform of the transient current pulse will be similar to the waveform of figure 12.

IV. SUMMARY

Discharges were observed to occur at a negatively biased array. The rate of discharge is proportional to the plasma density and to the biased voltage. The rate of discharge and the threshold voltage for the occurrence of discharge is also geometry dependent. The "PIX" array has a large area of exposed interconnects, and the interconnects have much sharper geometries than the "VOLT" array interconnects; consequently, the discharge rate of the "PIX"-type of array is higher than the rate of a "VOLT" array. The results suggest that the threshold discharge voltage of a high-voltage array can be lowered by the proper design of interconnect geometry.

The data displayed in figures 9 through 11 indicate that the RF generated by a discharge exceeds the emission level allowed by the shuttle. Therefore, the VOLT experiment should take precautions to control the possible adverse effects of discharge-generated RF. One possible solution is to install the solar array far away from sensitive electronic subsystems. The required distance depends on the susceptibility of the subsystems involved.

REFERENCES

1. Stevens N., "Interaction Between Large Space Power Systems and Low-Earth-Orbit Plasmas," Spacecraft Environmental Interactions Technology, 1983, NASA CP-2359, pp. 263, 1985.
2. Snyder D., "Discharges on a Negatively Biased Solar Cell Array in a Charge Particle Environment," ibid., pp. 379.
3. Leung P., "Discharge Characteristics of a Simulated Solar Cell Array," IEEE Transactions on Nuclear Science, Vol. NS-30, pp. 4311, 1983.
4. Konradi A., McIntyre B., and Potter A., "Experimental Studies of Scaling Laws for Plasma Collection at High Voltages," Journal of Spacecraft and Rockets, Vol. 21, No. 3, pp. 287, 1984.
5. Grier N., "Plasma Interaction Experiment II (PIX-II): Laboratory and Flight Results," Spacecraft Environmental Interaction Technology 1983, pp. 333, 1985.
6. Leung P. and Plamp G., "Characteristics of RF Resulting from Dielectric Discharges," IEEE Transactions on Nuclear Science, NS 29, pp. 1610-1614, 1982.
7. Bekefi G., "Radiation Process in Plasmas," Wiley, New York, 1980.
8. Grier N. and Stevens N., "Plasma Interaction Experiment (PIX) Flight Results," Spacecraft Charging Technology - 1978, NASA CP-2071, 1979, p. 295.
9. Carruth M. and Purvis C., "Space Test Program of High-Voltage Solar Array/Space Plasma Interactions," Spacecraft Environmental Interaction Technology 1983, pp. 619, 1985.
10. Interface Control Document (ICD 2-19001), Johnson Space Center.

TECHNICAL REPORT STANDARD TITLE PAGE

1. Report No. 85-82	2. Government Accession No.	3. Recipient's Catalog No.	
4. Title and Subtitle Characterization of EMI Generated by the Discharge of a "VOLT" Solar Array		5. Report Date November 1, 1985	6. Performing Organization Code
7. Author(s) Philip Leung		8. Performing Organization Report No.	
9. Performing Organization Name and Address JET PROPULSION LABORATORY California Institute of Technology 4800 Oak Grove Drive Pasadena, California 91109		10. Work Unit No.	11. Contract or Grant No. NAS7-918
12. Sponsoring Agency Name and Address NATIONAL AERONAUTICS AND SPACE ADMINISTRATION Washington, D.C. 20546		13. Type of Report and Period Covered JPL Publication	
15. Supplementary Notes		14. Sponsoring Agency Code RE65 DY-481-59-02-04-95	
16. Abstract The interaction of a high-voltage solar array with the space plasma environment is investigated in a laboratory simulation experiment. Discharges are observed to occur when the solar array is at a sufficiently high negative bias with respect to the plasma. The frequency of occurrence of discharge is found to depend critically on the plasma density and on the geometry of the array. The electromagnetic interference (EMI) associated with a discharge is also measured. The amplitude of EMI increases with the magnitude of the high voltage. Since the discharge-generated EMI is of significant amplitude, its effect on the performance of systems in space must be evaluated.			
17. Key Words (Selected by Author(s)) Aeronautics (General) Ground Support Systems and Facilities (Space) Spacecraft Propulsion and Power Quality Assurance and Reliability		18. Distribution Statement Unclassified; unlimited	
19. Security Classif. (of this report) Unclassified	20. Security Classif. (of this page) Unclassified	21. No. of Pages 24	22. Price